

ScienceDirect



IFAC PapersOnLine 56-2 (2023) 10222-10227

Multi-Layer Continuum Deformation Optimization of Multi-Agent Systems

Harshvardhan Uppaluru* Hossein Rastgoftar**

* Scalable Move And Resilient Traversability Lab, Aerospace and Mechanical Engineering department, University of Arizona, Tucson -85721, USA. Email: huppaluru@arizona.edu ** Scalable Move And Resilient Traversability Lab, Aerospace and Mechanical Engineering department, University of Arizona, Tucson -85721, USA. Email: hrastqoftar@arizona.edu

Abstract: This paper studies the problem of safe and optimal continuum deformation of a largescale multi-agent system (MAS). We present a novel approach for MAS continuum deformation coordination that aims to achieve safe and efficient agent movement using a leader-follower multi-layer hierarchical optimization framework with a single input layer, multiple hidden layers, and a single output layer. The input layer receives the reference (material) positions of the primary leaders, the hidden layers compute the desired positions of the interior leader agents and followers, and the output layer computes the nominal position of the MAS configuration. By introducing a lower bound on the major principles of the strain field of the MAS deformation, we obtain linear inequality safety constraints and ensure inter-agent collision avoidance. The continuum deformation optimization is formulated as a quadratic programming problem. It consists of the following components: (i) decision variables that represent the weights in the first hidden layer; (ii) a quadratic cost function that penalizes deviation of the nominal MAS trajectory from the desired MAS trajectory; and (iii) inequality safety constraints that ensure inter-agent collision avoidance. To validate the proposed approach, we simulate and present the results of continuum deformation on a large-scale quadcopter team tracking a desired helix trajectory, demonstrating improvements in safety and efficiency.

Copyright © 2023 The Authors. This is an open access article under the CC BY-NC-ND license (https://creativecommons.org/licenses/by-nc-nd/4.0/)

Keywords: Multi-agent systems, Flying robots, Networked robotic system modeling and control, Continuum Mechanics

1. INTRODUCTION

Coordination, formation control and cooperative control are important active areas of research in the field of Multi-Agent Systems(MAS) with a wide range of potential applications including, but not limited to, surveillance (Leslie et al., 2022), search and rescue operations (Kleiner et al., 2013), and air traffic monitoring (Idris et al., 2018). In terms of efficiency, costs, and resilience to failure, a MAS comprised of Unmanned Aerial Vehicles (UAV) can provide substantial benefits over a single UAV. Cooperation among MAS agents improves the multi-agent team's capacity to recover from abnormalities. Virtual structure, containment control, consensus control and continuum deformation (Rastgoftar, 2016) are some of the prominent and existing approaches for multi-agent system coordination that have been extensively studied.

1.1 Related Work

The centralized coordination approach in which the multiagent formation is represented as a single structure and a rigid body is known as Virtual Structure (Lewis and Tan, 1997: Beard et al., 2000). Given some orientation in 3-D motion space, the virtual structure moves in a certain direction as a rigid body while maintaining the rigid geometric relationship between multiple agents. Consensus control (Cao et al., 2015; Shao et al., 2018) is a decentralized technique with various coordination implementations presented such as leaderless multi-agent consensus (Ding et al., 2019; Qin et al., 2016) and leader-follower consensus (Wu et al., 2018). Another decentralized leader-follower technique is containment control (Notarstefano et al., 2011), where a fixed number of leaders guide the followers via local communication. A multi-agent system's finitetime containment control has been investigated (Wang et al., 2013; Liu et al., 2015). The criteria required and adequate for containment control stability and convergence were developed in (Cao et al., 2012; Ji et al., 2008). Researchers investigated containment control in the context of fixed and switching inter-agent communication (Li et al., 2015).

Continuum deformation (Rastgoftar, 2016; Rastgoftar and Atkins, 2017; Uppaluru et al., 2022) is a decentralized multi-agent coordination technique that considers agents as finite number of particles in a continuum that deform and translate in 3-D space. An n-D (n = 1, 2, 3) continuum deformation coordination has at least n + 1 leaders in \mathbb{R}^n ,

^{*} This work has been supported by the National Science Foundation under Award Nos. 2133690 and 1914581.

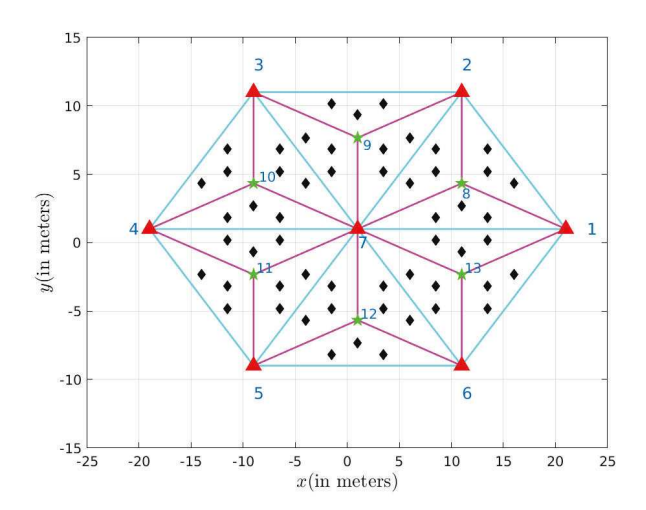


Fig. 1. An example of the configuration of a N=67 agent team defined by set $\mathcal{V}=\{1,\cdots,67\}$, where $\mathcal{V}=\mathcal{W}_1\bigcup\mathcal{W}_2\bigcup\mathcal{W}_3$. The set $\mathcal{W}_1=\{1,\cdots,7\}$ is represented by red triangles where 1 through 6 are the boundary leader agents and 7 is the core leader agent. Set $\mathcal{W}_2=\mathcal{W}_1\cup\{8,\cdots,13\}$, set $\mathcal{W}_3=\mathcal{W}_2\cup\{14,\cdots,67\}$ identifies all the agents in the N-agent configuration. We also define the set $\mathcal{T}=\{1,\cdots,6\}$ that identifies the number of unique triangles formed by the leading polygon. Set \mathcal{V}_j associates particular agents enclosed by triangle $j\in\mathcal{T}$.

positioned at the vertices of an n-D simplex at any time t. Leaders plan the agent team's continuum deformation independently which are acquired by followers through local communication. Despite the fact that both containment control and continuum deformation are decentralized leader-follower approaches, continuum deformation enables inter-agent collision avoidance, obstacle collision avoidance, and agent containment by formally specifying and verifying safety in a large-scale multi-agent coordination (Rastgoftar et al., 2018; Rastgoftar and Atkins, 2019). A large scale multi-agent system can safely and aggressively deform in an obstacle-filled environment by employing continuum deformation coordination. Experimental evaluation of continuum deformation coordination in 2-D with a team of quadcopters has been performed previously (Romano et al., 2019, 2022; Uppaluru and Rastgoftar, 2022).

1.2 Contributions and Outline

We advance the existing continuum deformation approach (Rastgoftar, 2016; Rastgoftar and Atkins, 2017; Uppaluru et al., 2022) towards multi-layer continuum deformation (MLCD) coordination at which the desired multi-agent deformation is planned by a finite number of leaders organized hierarchically through a feed-forward network. The feed-forward hierarchical network consists of one input layer receiving reference positions of the boundary agents, p hidden layers, and one output layer. While the first p-1 hidden layers contain neurons that represent leaders, the neurons sorted in the last hidden layer (hidden layer p) all represent follower agents. The output layer computes nominal position of the agent team configuration by minimizing the error between nominal and desired trajectories.

The proposed MLCD overcomes the deformation uniformity of the available continuum deformation coordination, which is resulted from deformation planning by a single Jacobian matrix. MLCD is defined as a quadtratic programming problem with inequality safety constraints obtained by eigen-decomposition of MAS spatial deformation matrices.

The rest of the paper is organized as follows: Preliminaries are first introduced in Section 2 followed by a detailed description of our approach in Section 3. Safety guarantee conditions have been presented in Section 4 before presenting simulation results in Section 5. Section 6 concludes the paper.

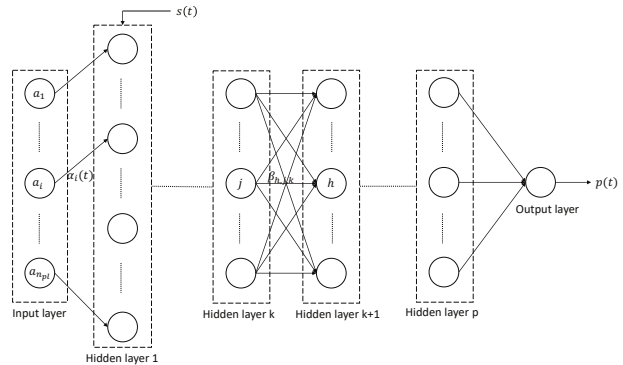


Fig. 2. The structure of the proposed hierarchical optimization approach inspired from neural networks.

2. PRELIMINARIES

We define a N-agent team as individual particles of a deforming body navigating collectively in a 3-D motion space. An example of the N-agent team configuration where N=67 is shown in Figure 1. The set $\mathcal{V}=\{1,\cdots,N\}$ is used to uniquely identify all the agents in the team. Set \mathcal{V} can be expressed as

$$\mathcal{V} = \bigcup_{k=1}^{p} \mathcal{W}_k \tag{1}$$

with subsets W_1 through W_p , where W_1 defines the boundary leader agents and a single core (leader) agent located inside the agent team configuration; W_2 through W_{p-1} define the interior leaders; and W_p defines pure follower agents. The boundary and core agents defined by W_1 are called *primary leaders* and $n_{pl} = |W_1|$ denotes the number of primary leaders.

Subset W_k functions as immediate leaders for W_{k+1} (for $k = 1, \dots, p-1$), which implies that desired positions of the agents belonging to W_{k+1} are obtained based upon the desired positions of the agents in W_k . Explicitly, the desired position of agent $i \in W_{k+1}$ is given by

$$\mathbf{p}_{i}(t) = \sum_{j \in \mathcal{W}_{k}} \beta_{i,j,k} \mathbf{p}_{j}(t), \quad k = 2, \cdots, p - 1, \quad (2)$$

where $\beta_{i,j,k} \in [0,1]$, and

$$\sum_{j \in \mathcal{W}_k} \beta_{i,j,k} = 1, \qquad i \in \mathcal{W}_{k+1}, \ k = 2, \cdots, p-1.$$
 (3)

The desired trajectories of agents belonging to set W_1 are calculated using

$$\mathbf{p}_l(t) = \alpha_l(t)\mathbf{a}_{l0} + \mathbf{s}(t), \qquad \forall l \in \mathcal{W}_1, \tag{4}$$

where $\alpha_l(t)$ is a positive weight parameter $\in [\alpha_{min}, \alpha_{max}],$ \mathbf{a}_{l0} specifies the constant reference (material) position of agents $l \in \mathcal{W}_1$ at time t_0 , $\mathbf{s}(t)$ is the desired position of the N-agent team configuration with respect to an inertial coordinate system. Note that the reference position of the core agent $l \in \mathcal{W}_1$ is $\mathbf{0}$, i.e. $\mathbf{a}_{n_{nl}} = \mathbf{0}$.

Assumption 1. We assume that the magnitude of reference position of every boundary leader $l \in \mathcal{W}_1 \setminus \{n_{pl}\}$ is the same and it is equal to a_0 . Therefore,

$$\bigwedge_{l \in \mathcal{W}_1 \setminus \{n_{pl}\}} (\|\mathbf{a}_{l0}\| = a_0). \tag{5}$$

3. PROPOSED APPROACH

We propose a hierarchical optimization framework for safe and optimal continuum deformation coordination of a N-agent team over the finite time interval $[t_0, t_f]$. The proposed hierarchical structure resembles a Neural Network (See Figure. 2) and consists of one input layer, hidden layers, and a single output layer, where the nodes contained by non-output layers represent agents. The hierarchical framework is structured as follows:

As shown in Figure. 2, the input layer receives the timeinvariant reference (material) position (\mathbf{a}_{l0}) of primary leader agents at time t_0 . The first hidden layer computes the desired trajectories of boundary and core agents using equation (4). More specifically, in hidden layer 1, node $j \in \mathcal{W}_1$, receives reference position \mathbf{a}_{i0} , and bias $\mathbf{s}(t)$, to return $\mathbf{p}_i(t)$ according to equation (4). The weights associated with this hidden layer are coined as $\alpha(t)$. Every hidden layer $k \in \{2, \dots, p\}$ acquires desired positions from previous hidden layer k-1 and yields the desired positions of the agents defined by W_k by using Eq. (2). Note that bias is $\mathbf{0}$ in these hidden layers 2 through p. The weights associated with hidden layer $k \in \{2, \dots, p\}$ is coined as β_k and are constant.

The output layer generates the nominal position of Nagent team configuration which is denoted by $\mathbf{p}(t)$ by averaging the desired positions of agents in \mathcal{W}_p . Note that $\mathbf{p}(t)$ is the nominal position of N-agent team configuration at any time $t \in [t_0, t_f]$.

3.1 Continuum Deformation Optimization

Our objective is to determine the time-varying factors $\alpha_l(t)$, used in Eq. (4), for every $l \in \mathcal{W}_1$ and any $t \in [t_0, t_f]$ by applying quadratic programming, assuming that $\boldsymbol{\beta}_k = \left[\boldsymbol{\beta}_{i,j,k}\right] \in \mathbb{R}^{|\mathcal{W}_k| \times |\mathcal{W}_{k-1}|}$ is constant for $k \in \{2, \cdots, p\}$, where $|\cdot|$ denotes set cardinality. To this end, we aim to minimize the deviation of the nominal position of N-agent team configuration, denoted by $\mathbf{p}(t) = [p_x(t), p_y(t), p_z(t)]^T$, from the desired position $\mathbf{s}(t) = \left[s_x(t), s_y(t), s_z(t)\right]^T$, at any time t, where the nominal position $\mathbf{p}(t)$ is calculated using the following equation:

$$\mathbf{p}(t) = \begin{bmatrix} p_x(t) \\ p_y(t) \\ p_z(t) \end{bmatrix} = \frac{1}{N_p} \sum_j \mathbf{p}_j(t) \qquad \forall j \in \mathcal{W}_p \qquad (6)$$

where $N_p = |\mathcal{W}_p|$ denotes the cardinality of the set \mathcal{W}_p . Before further discussion, we first define $\alpha(t)$ as

$$\boldsymbol{\alpha}(t) = \begin{bmatrix} \alpha_1(t) & 0 & \dots & 0 \\ 0 & \alpha_2(t) & \dots & 0 \\ \vdots & \vdots & \ddots & \vdots \\ 0 & 0 & \dots & \alpha_{n_n}(t) \end{bmatrix}$$
(7)

Given material position of leader l as

$$\mathbf{a}_{l0} = \left[\mathbf{a}_{l0x} \ \mathbf{a}_{l0y} \ \mathbf{a}_{l0z} \right]^T, \qquad \forall l \in \mathcal{W}_1, \tag{8}$$

we define the following diagonal matrices:

$$\mathbf{a}_{0x} = \begin{bmatrix} a_{10x} & & & \\ & \ddots & & \\ & & a_{n_{pl}0x} \end{bmatrix} \in \mathbb{R}^{n_{pl} \times n_{pl}}, \qquad (9)$$

$$\mathbf{a}_{0y} = \begin{bmatrix} a_{10y} & & & \\ & \ddots & & \\ & & a_{n_{pl}0y} \end{bmatrix} \in \mathbb{R}^{n_{pl} \times n_{pl}}, \qquad (10)$$

$$\mathbf{a}_{0z} = \begin{bmatrix} a_{10z} & & & \\ & \ddots & & \\ & & a_{n_{pl}0z} \end{bmatrix} \in \mathbb{R}^{n_{pl} \times n_{pl}}. \qquad (11)$$

Furthermore, we define matrices $\Delta_x, \Delta_y, \Delta_z$ as follows:

$$\Delta_x = \frac{1}{N_p} \mathbf{1}_{(1 \times N_p)} \boldsymbol{\beta}_p \cdots \boldsymbol{\beta}_2 \mathbf{a}_{0x} \in \mathbb{R}^{1 \times n_{pl}}, \qquad (12)$$

$$\mathbf{\Delta}_{y} = \frac{1}{N_{p}} \mathbf{1}_{(1 \times N_{p})} \boldsymbol{\beta}_{p} \cdots \boldsymbol{\beta}_{2} \mathbf{a}_{0y} \in \mathbb{R}^{1 \times n_{pl}}, \qquad (13)$$

$$\Delta_z = \frac{1}{N_p} \mathbf{1}_{(1 \times N_p)} \boldsymbol{\beta}_p \cdots \boldsymbol{\beta}_2 \mathbf{a}_{0z} \in \mathbb{R}^{1 \times n_{pl}}.$$
 (14)

Using the definitions above, and by defining the state vector $\mathbf{X} = \left[\alpha_1, \cdots, \alpha_{n_{pl}}, s_x, s_y, s_z\right]^T \in \mathbb{R}^{(n_{pl}+3)\times 1}$, we write individual components of nominal position $\mathbf{p}(t)$ as

$$p_x(t) = [\mathbf{\Delta}_x \ 1 \ 0 \ 0] \mathbf{X}(t) = \mathbf{R}_X \mathbf{X}(t) \tag{15}$$

$$p_y(t) = \left[\mathbf{\Delta}_y \ 0 \ 1 \ 0 \right] \mathbf{X}(t) = \mathbf{R}_Y \mathbf{X}(t) \tag{16}$$

$$p_z(t) = \left[\mathbf{\Delta}_z \ 0 \ 0 \ 1 \right] \mathbf{X}(t) = \mathbf{R}_Z \mathbf{X}(t) \tag{17}$$

where \mathbf{R}_X , \mathbf{R}_Y , \mathbf{R}_Z are of shape $(1, n_{nl} + 3)$.

The objective of the quadratic programming problem is assign X by solving the following optimization problem:

$$\underset{\mathbf{X}}{\text{minimize}} \quad \frac{1}{2} \mathbf{X}^T \mathbf{H} \mathbf{X} + \mathbf{k}^T \mathbf{X} \tag{18}$$

subject to the following inequality and equality constraints:

$$\mathbf{A}_{ineq}\mathbf{X} \le \mathbf{B}_{ineq}, \tag{19a}$$
$$\mathbf{A}_{eq}\mathbf{X} = \mathbf{B}_{eq}(t), \tag{19b}$$

(19b)

where

$$\mathbf{A}_{ineq} = \begin{bmatrix} -\mathbf{I}_{(n_{pl}-1)\times(n_{pl}-1)} & \mathbf{0}_{(n_{pl}-1)\times4} \\ \mathbf{I}_{(n_{pl}-1)\times(n_{pl}-1)} & \mathbf{0}_{(n_{pl}-1)\times4} \end{bmatrix}$$
(20)

$$\mathbf{B}_{ineq} = \begin{bmatrix} -\alpha_{min} \times \mathbf{1}_{(n_{pl}-1)\times 1} \\ \alpha_{max} \times \mathbf{1}_{(n_{pl}-1)\times 1} \end{bmatrix}$$
 (21)

$$\mathbf{A}_{eq} = \begin{bmatrix} \mathbf{0}_{4 \times (n_{pl} - 1)} & \mathbf{diag}[1, 1, 1, 1] \end{bmatrix}$$
 (22)

$$\mathbf{B}_{eq}(t) = \begin{bmatrix} 0 \\ s_x(t) \\ s_y(t) \\ s_z(t) \end{bmatrix}$$
 (23)

$$\mathbf{H} = \zeta \mathbf{I}_{(n_{pl}+3)\times(n_{pl}+3)} + \mathbf{R}_X^T \mathbf{R}_X + \mathbf{R}_Y^T \mathbf{R}_Y + \mathbf{R}_Z^T \mathbf{R}_Z \quad (24)$$

$$\mathbf{k}^T = -2(s_x \mathbf{R}_X + s_y \mathbf{R}_Y + s_z \mathbf{R}_z) \tag{25}$$

 $\mathbf{k}^{T} = -2(s_x \mathbf{R}_X + s_y \mathbf{R}_Y + s_z \mathbf{R}_z)$ (25) $\mathbf{I}_{(n_{pl}-1)\times(n_{pl}-1)} \in \mathbb{R}^{(n_{pl}-1)\times(n_{pl}-1)} \text{ is an identity matrix}$ and $\mathbf{0}_{(n_{pl}-1)\times 4} \in \mathbb{R}^{(n_{pl}-1)\times 4}$ is a matrix of zeros in Eq.

(20). Also, $\mathbf{1}_{(n_{pl}-1)\times 1} \in \mathbb{R}^{(n_{pl}-1)\times 1}$ represents a vector of ones in Eq. (21). In Eq. (24), $\zeta > 0$ is a small positive number and $\mathbf{I}_{(n_{pl}+3)\times(n_{pl}+3)} \in \mathbb{R}^{(n_{pl}+3)\times(n_{pl}+3)}$ is an identity matrix. α_{min} and α_{max} are the minimum and maximum values of $\alpha_l(t)$.

4. SAFETY CONDITIONS

To ensure safety of the multi-agent team continuum deformation, we provide inter-agent collision avoidance and agent containment conditions by determining α_{min} and α_{max} as discussed in sections 4.1 and 4.2 below.

4.1 Collision Avoidance

The desired configuration of the agent team is contained by the leading polygon consisting of $n_{pl}-1$ triangles that are defined by the set $\mathcal{T} = \{1, \dots, n_{pl} - 1\}$. We can express set \mathcal{V} as

$$\mathcal{V} = \bigcup_{j \in \mathcal{T}} \mathcal{V}_j,\tag{26}$$

where V_i identifies particular agents enclosed by triangular cell $j \in \mathcal{T}$. Because desired trajectories of the agents are defined by piece-wise affine transformations in Eqs. (2) and (4), the desired position of agent $i \in \mathcal{V}_i$ can be given by

$$\mathbf{p}_{i}(t) = \mathbf{Q}_{i}(t)\mathbf{a}_{i0} + \mathbf{b}_{i}, \qquad j \in \mathcal{T}, \ i \in \mathcal{V}_{i}$$
 (27)

 $\mathbf{p}_{i}(t) = \mathbf{Q}_{j}(t)\mathbf{a}_{i0} + \mathbf{b}_{j}, \quad j \in \mathcal{T}, \ i \in \mathcal{V}_{j} \quad (27)$ with nonsingular Jacobian matrix $\mathbf{Q}_{j} \in \mathbb{R}^{3\times3}$ and rigid-body displacement vector $\mathbf{b}_{j} \in \mathbb{R}^{3\times1}$, where \mathbf{a}_{i0} is the reference position of agent $i \in \mathcal{V}_i$.

We denote $\lambda_{1,j}(t)>0,\ \lambda_{2,j}(t)>0,\ {\rm and}\ \lambda_{3,j}(t)$ as the eigenvalues of pure deformation matrix $\mathbf{U}_j(t)=0$ $(\mathbf{Q}_j(t)^T\mathbf{Q}_j(t))^{\frac{1}{2}}$, and make the following assumptions: Assumption 2. Every agent i can be enclosed by a ball of radius ϵ .

Assumption 3. Every agent i can stably track the desired trajectory $\mathbf{p}_{i}(t)$ such that the tracking error does not exceed δ . This implies that

$$\|\mathbf{r}_i(t) - \mathbf{p}_i(t)\| \le \delta, \quad \forall t$$
 (28)

where $\mathbf{r}_{i}(t)$ and $\mathbf{p}_{i}(t)$ denote the actual and desired positions of agent $i \in \mathcal{V}$ at time t.

By evoking the theorem developed in Ref. (Rastgoftar and Kolmanovsky (2021)), inter-agent collision avoidance is assured in $j \in \mathcal{T}$, if

$$\min \left\{ \lambda_{1,j}(t), \lambda_{2,j}(t), \lambda_{3,j}(t) \right\} \ge \frac{2 \left(\delta + \epsilon \right)}{p_{\min,j}}, \qquad j \in \mathcal{T}, \ \forall t,$$
(29)

where $p_{min,j}$ is the minimum separation distance between every two agents inside $j \in \mathcal{T}$. Then, inter-agent collision avoidance between every two agents in $\mathcal V$ is assured, if

$$\alpha_{min} = \max_{j \in \mathcal{T}} \frac{2(\delta + \epsilon)}{p_{min,j}} \tag{30}$$

assigns a lower bound on $\alpha_i(t)$ for every $i \in \mathcal{W}_1$ at any time t.

4.2 Agent Containment

We can assure that every agent remains inside a ball of radius a_{max} , if

$$\alpha_{max} = \frac{a_{max} - 2(\delta + \epsilon)}{a_0} \tag{31}$$

where a_0 is the reference position of boundary leaders' (See Assumption 1). Also, δ is the control tracking error bound and ϵ is radius of the circle enclosing every agent i, as they were introduced in Section 4.1.

5. SIMULATIONS

The simulations for this study were conducted on a desktop computer equipped with an Intel i7 11-th gen CPU, 16 GB of RAM, and running MATLAB R2022b on Ubuntu 20.04. We investigated the evolution of a multi-quadcopter system (MQS) consisting of N = 67 quadcopters, which were assumed to have similar size and attributes. The quadcopters' dynamics were modelled based on the work by Rastgoftar (2022) (Rastgoftar, 2022) and the quadcopter parameters can be found in Gopalakrishnan (2017) (Gopalakrishnan, 2017).

The quadcopters are identified by unique index numbers defined by the set $\mathcal{V} = \{1, \dots, 67\}$ with primary leader quadcopters defined by $W_1 = \{1, \dots, 7\}$. The interior leader quadcopter are given by the set $W_2 = \{8, \dots, 13\}$ and the followers are denoted uniquely using the set $\mathcal{W}_3 = \{14, \cdots, 67\}$. Therefore, for this simulation we have p=3. The minimum and maximum values assigned for the weights $\alpha(t)$ are in the range [0.6, 5.0]. The objective is to determine these weights using Quadratic Programming such that inter-quadcopter collision avoidance is guaranteed (See Section 4) in the MQS.

For time t in the range [0,T], the large-scale quadcopter team is supposed to move in an obstacle-free environment from an initial configuration, shown in Figure 1, until final time T is reached while tracking the desired helix trajectory. The desired helix trajectory (Lee et al., 2010) is generated as follows:

$$\mathbf{s}(t) = \begin{bmatrix} s_x(t) \\ s_y(t) \\ s_z(t) \end{bmatrix} = \begin{bmatrix} 0.4\omega t \\ 0.4\sin(\pi\omega t) \\ 0.6\cos(\pi\omega t) \end{bmatrix}$$
(32)

where $\omega = 0.01$ and T = 1000 s. The reference (material) positions of the primary leaders are given by

$$\begin{bmatrix} \mathbf{a}_{10x} & \cdots & \mathbf{a}_{n_{pl}0x} \\ \mathbf{a}_{10y} & \cdots & \mathbf{a}_{n_{pl}0y} \\ \mathbf{a}_{10z} & \cdots & \mathbf{a}_{n_{pl}0z} \end{bmatrix} = \begin{bmatrix} 20 & 10 & -10 & -20 & -10 & 10 & 0 \\ 0 & 10 & 10 & 0 & -10 & -10 & 0 \\ -1 & 1 & 1 & -1 & 1 & 1 & 0 \end{bmatrix}$$
(33)

In our MATLAB simulations, the state vector \mathbf{X} is defined as $\mathbf{X} = [\alpha_1, \alpha_2, \alpha_3, \alpha_4, \alpha_5, \alpha_6, \alpha_7, s_x, s_y, s_z]^T$. From equation (24), we observe that **H** depends on constant weights $\beta_{i,j,k}$ for $k = \{2, \dots, p\}$ and constant reference (material) configuration \mathbf{a}_{l0} . Therefore, **H** is constant for all time t. However \mathbf{k}^T depends on time-varying desired trajectory $\mathbf{s}(t)$. In Figure 4, optimal values of $\alpha(t)$ obtained through quadratic programming have been plotted. Using inputoutput feedback linearization control approach (Rastgoftar, 2022), Figure 5 plots x-position component, y-position component, z-position component, rotors' angular speeds and thrust force magnitude of quadcopter $67 \in \mathcal{W}_3$, respectively.

6. CONCLUSION

This paper has developed and presented a leader-follower model for large-scale safe and optimal continuum deformation coordination by formulating the optimization as

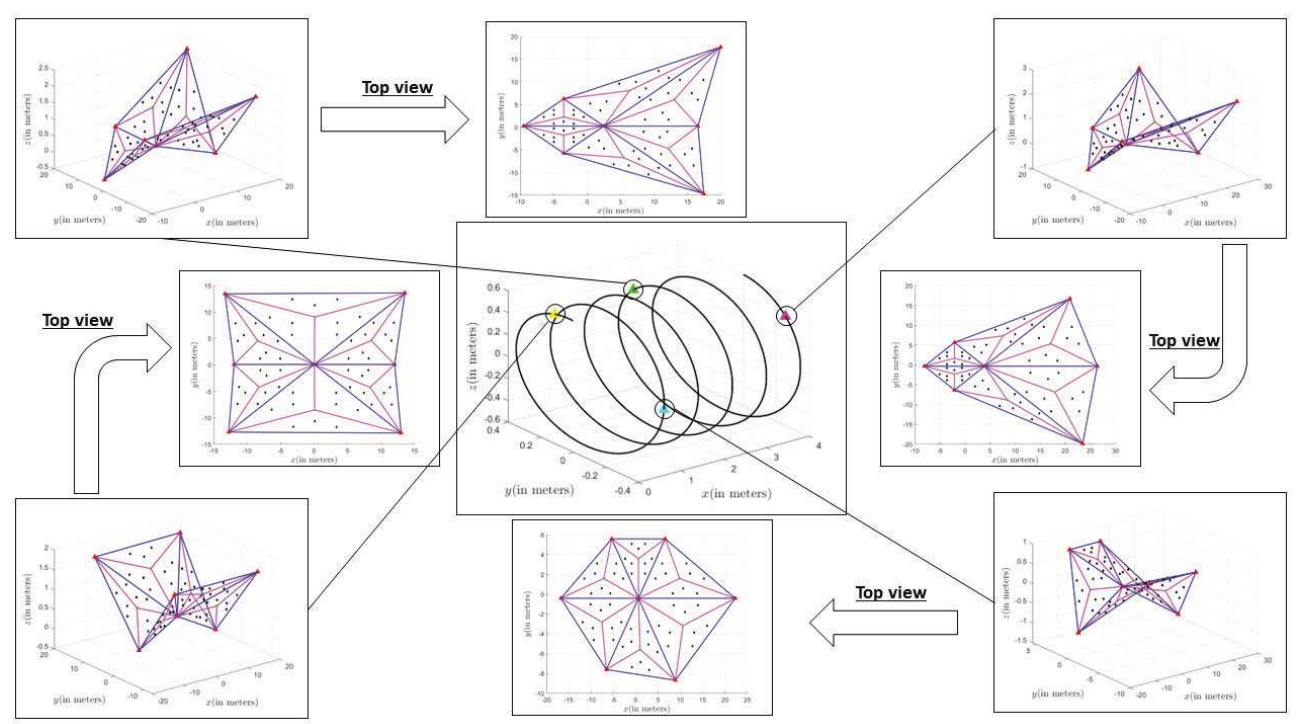


Fig. 3. Configurations of the MQS at various times while tracking the desired helix trajectory.

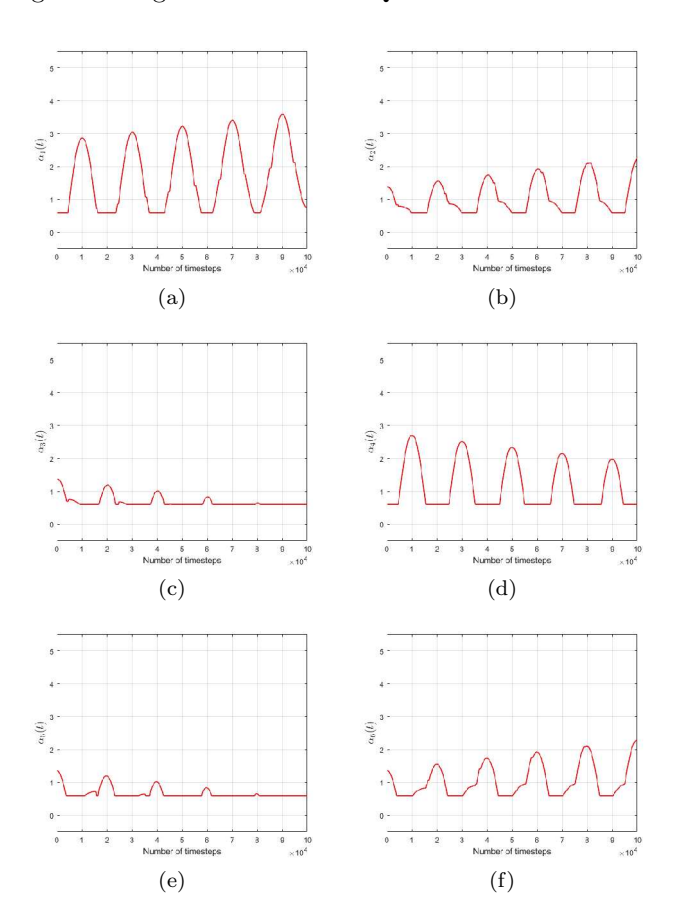


Fig. 4. $\alpha(t)$ for simple helical path

quadratic programming problem. We take inspiration from graphical structure of a neural network to develop a hierarchical optimization framework and obtain time-varying weights over time $t \in [t_0, t_f]$ using constant reference

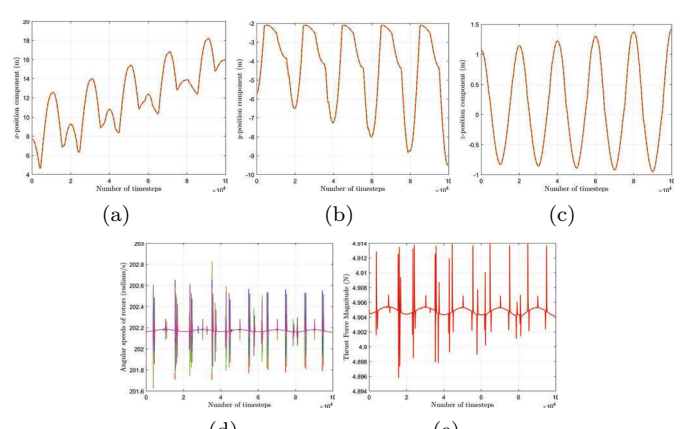


Fig. 5. (a) Desired (green) vs Actual (red) x-position component, (b) Desired (green) vs Actual (red) y-position component, (c) Desired (green) vs Actual (red) z-position component, (d) Angular speeds of rotors, (e) Thrust force magnitude for quadcopter agent 67.

(material) configuration of the agents as the input. We also provided conditions to assure safety between every two agents while the desired trajectory is tracked by the nominal position of the MAS with minimal deviation. As implied by our simulation results, our approach consisting of N=67 quadcopters is able to track a known target trajectory in 3-D motion space. Future work in this area can be further extended by making the algorithm more robust as follows: (1) by extending the approach to an obstacle-laden environment integrated with path-planning algorithms such as A^* ; (2) integrate our previously proposed fluid flow navigation function (Uppaluru et al., 2022; Romano et al., 2022; Emadi et al., 2022) as an obstacle-avoidance algorithm to account for sudden and abrupt failures in the multi-agent system (MAS); and (3) conduct

flight experiments to pass through a different windows of known shape and size.

REFERENCES

- Beard, R.W., Lawton, J., and Hadaegh, F.Y. (2000). A feedback architecture for formation control. In Proceedings of the 2000 American Control Conference. ACC (IEEE Cat. No. 00CH36334), volume 6, 4087–4091. IEEE.
- Cao, W., Zhang, J., and Ren, W. (2015). Leader–follower consensus of linear multi-agent systems with unknown external disturbances. Systems & Control Letters, 82, 64–70.
- Cao, Y., Ren, W., and Egerstedt, M. (2012). Distributed containment control with multiple stationary or dynamic leaders in fixed and switching directed networks. *Automatica*, 48(8), 1586–1597.
- Ding, C., Dong, X., Shi, C., Chen, Y., and Liu, Z. (2019). Leaderless output consensus of multi-agent systems with distinct relative degrees under switching directed topologies. *IET Control Theory & Applications*, 13(3), 313–320.
- Emadi, H., Uppaluru, H., and Rastgoftar, H. (2022). A physics-based safety recovery approach for fault-resilient multi-quadcopter coordination. In 2022 American Control Conference (ACC), 2527–2532. IEEE.
- Gopalakrishnan, E. (2017). Quadcopter flight mechanics model and control algorithms. Czech Technical University, 69.
- Idris, H., Bilimoria, K., Wing, D., Harrison, S., and Baxley, B. (2018). Air traffic management technology demonstration—3 (atd-3) multi-agent air/ground integrated coordination (maagic) concept of operations. Technical report, NASA/TM-2018-219931, NASA, Washington DC.
- Ji, M., Ferrari-Trecate, G., Egerstedt, M., and Buffa, A. (2008). Containment control in mobile networks. *IEEE Transactions on Automatic Control*, 53(8), 1972–1975.
- Kleiner, A., Farinelli, A., Ramchurn, S., Shi, B., Maffioletti, F., and Reffato, R. (2013). Rmasbench: benchmarking dynamic multi-agent coordination in urban search and rescue. In 12th International Conference on Autonomous Agents and Multiagent Systems (AAMAS 2013), 1195–1196. The International Foundation for Autonomous Agents and Multiagent Systems
- Lee, T., Leok, M., and McClamroch, N.H. (2010). Geometric tracking control of a quadrotor uav on se (3). In 49th IEEE conference on decision and control (CDC), 5420–5425. IEEE.
- Leslie, E., Flint, S., Briggs, H.C., Anderson, M.L., Appel, G., Konig, S., Bowen, N., Foster, C., Ganesh, P., and Ramos, H. (2022). An unmanned system for persistent surveillance in gps-denied environments. In AIAA SCITECH 2022 Forum, 0118.
- Lewis, M.A. and Tan, K.H. (1997). High precision formation control of mobile robots using virtual structures. *Autonomous robots*, 4(4), 387–403.
- Li, W., Xie, L., and Zhang, J.F. (2015). Containment control of leader-following multi-agent systems with markovian switching network topologies and measurement noises. *Automatica*, 51, 263–267.
- Liu, H., Cheng, L., Tan, M., Hou, Z., and Wang, Y. (2015). Distributed exponential finite-time coordination

- of multi-agent systems: containment control and consensus. *International Journal of Control*, 88(2), 237–247.
- Notarstefano, G., Egerstedt, M., and Haque, M. (2011). Containment in leader–follower networks with switching communication topologies. *Automatica*, 47(5), 1035–1040.
- Qin, J., Yu, C., and Anderson, B.D. (2016). On leaderless and leader-following consensus for interacting clusters of second-order multi-agent systems. *Automatica*, 74, 214–221.
- Rastgoftar, H. (2016). Continuum deformation of multiagent systems. Springer.
- Rastgoftar, H. (2022). Real-time deployment of a large-scale multi-quadcopter system (mqs). arXiv preprint arXiv:2201.10509.
- Rastgoftar, H. and Atkins, E.M. (2017). Continuum deformation of multi-agent systems under directed communication topologies. *Journal of Dynamic Systems*, *Measurement*, and Control, 139(1).
- Rastgoftar, H. and Atkins, E.M. (2019). Safe multi-cluster uav continuum deformation coordination. *Aerospace Science and Technology*, 91, 640–655.
- Rastgoftar, H., Atkins, E.M., and Panagou, D. (2018). Safe multiquadcopter system continuum deformation over moving frames. *IEEE Transactions on Control of Network Systems*, 6(2), 737–749.
- Rastgoftar, H. and Kolmanovsky, I.V. (2021). Safe affine transformation-based guidance of a large-scale multi-quadcopter system (mqs). *IEEE Transactions on Control of Network Systems*.
- Romano, M., Kuevor, P., Lukacs, D., Marshall, O., Stevens, M., Rastgoftar, H., Cutler, J., and Atkins, E. (2019). Experimental evaluation of continuum deformation with a five quadrotor team. In 2019 American Control Conference (ACC), 2023–2029. IEEE.
- Romano, M., Uppaluru, H., Rastgoftar, H., and Atkins, E. (2022). Quadrotor formation flying resilient to abrupt vehicle failures via a fluid flow navigation function. arXiv preprint arXiv:2203.01807.
- Shao, J., Zheng, W.X., Huang, T.Z., and Bishop, A.N. (2018). On leader–follower consensus with switching topologies: An analysis inspired by pigeon hierarchies. *IEEE Transactions on Automatic Control*, 63(10), 3588–3593.
- Uppaluru, H., Emadi, H., and Rastgoftar, H. (2022). Resilient multi-uas coordination using cooperative localization. *Aerospace Science and Technology*, 131, 107960. doi:https://doi.org/10.1016/j.ast.2022.107960.
- Uppaluru, H. and Rastgoftar, H. (2022). Drones practicing mechanics. arXiv preprint arXiv:2201.08004.
- Wang, X., Li, S., and Shi, P. (2013). Distributed finite-time containment control for double-integrator multiagent systems. *IEEE Transactions on Cybernetics*, 44(9), 1518–1528.
- Wu, Y., Wang, Z., Ding, S., and Zhang, H. (2018). Leader-follower consensus of multi-agent systems in directed networks with actuator faults. *Neurocomputing*, 275, 1177–1185.